

On the theory of difference frequency generation and light rectification in the scanning tunnelling microscope

This article has been downloaded from IOPscience. Please scroll down to see the full text article.

1992 J. Phys.: Condens. Matter 4 7341

(<http://iopscience.iop.org/0953-8984/4/36/009>)

[View the table of contents for this issue](#), or go to the [journal homepage](#) for more

Download details:

IP Address: 171.66.16.96

The article was downloaded on 11/05/2010 at 00:30

Please note that [terms and conditions apply](#).

On the theory of difference frequency generation and light rectification in the scanning tunnelling microscope

A Levy Yeyati and F Flores

Departamento de Física de la Materia Condensada CXII, Universidad Autónoma de Madrid, E-28049 Madrid, Spain

Received 28 May 1992

Abstract. The problem of currents induced in the scanning tunnelling microscope due to incident laser radiation is analysed. We use a tight-binding description of the microscope tunnelling junction, and the interaction with the laser field is taken into account by an effective time-dependent coupling between tip and sample. The currents generated at frequencies that are linear combinations of the incident frequencies are then obtained with the help of a non-equilibrium Green's function formalism. Particular attention is paid to the rectification and difference frequency generation effects. In this work we extend previous results for the rectified current to the case where a direct bias is applied in addition to the laser field. It is shown that in the limit of very low frequencies the dynamical response may be deduced from the static characteristic curve. In order to compare with recent experimental data, we perform model calculations for a graphite sample and study the induced photocurrent as a function of bias voltage, tip-sample distance and photon energy. The limitations of the adiabatic approximation are discussed. Finally, we present results for the rectified current in the presence of an adsorbed molecule with a characteristic vibrational mode. The contribution from inelastic processes is obtained to the lowest order in the electron-phonon coupling. It is shown that the onset of inelastic tunnelling should be reflected as a singularity in the rectified current as a function of both bias voltage and photon energy.

1. Introduction

Between the new modes of operation of the scanning tunnelling microscope (STM) developed in recent years, there is a growing interest to those methods in which the device is driven by laser radiation [1, 2, 3, 4]. The aim of these investigations is the development of a new tool for the detection and identification of adsorbates, as well as for the analysis of surface-specific excitations.

For this purpose it is important to understand the basic facts associated with the interaction between laser radiation and tunnelling electrons at the tip-sample interface. Recent experimental evidence [3] shows that the observation of large second-order effects like rectification and second-harmonic generation can be related to non-linearities in the current-voltage characteristic. The same group has demonstrated by using two laser beams of different frequencies the possibility of generating a signal in the difference frequency [1, 3], and has used it to obtain atomic resolution images of the graphite surface [4].

Regarding the problem about the frequency limit in the dynamical response of the STM, it has been claimed [5] that light rectification in STM might be used to

measure the electron tunnelling time by detecting a cut-off frequency. Estimates of this time are in the order of 10^{-14} s for a triangular barrier [6]. The observation of light rectification at frequencies as large as 30 THz [4, 3], however, casts doubts on the existence of a clear cut-off in the dynamical response. This point will be addressed later in light of our present approach.

In a previous work [7] (hereafter referred to as I) we have proposed a model for analysing a STM junction in the presence of an AC photon field. The electrons were described by a tight-binding Hamiltonian and the coupling with the laser field was included via a time-dependent part in the hopping elements. With the help of a non-equilibrium Green's function technique introduced by Keldysh [8] we obtained a closed expression for the DC current (hereafter called rectified current) induced by the laser radiation when no DC bias is applied. Here we extend this work to the case of a non-zero bias. This requires the inclusion of higher-order terms in the effective time-dependent coupling between the tip and the sample, that are obtained by using very general arguments for the coupling with an electromagnetic (EM) field.

On the other hand, we present results for the difference frequency generation and show how its signal is related to the rectified current.

One of the aims of this work is also to determine up to which extent the dynamical behaviour of the STM may be known from the static I - V characteristic. To this end we perform model calculations for a tungsten tip and a graphite sample, and study the behaviour of the rectified current as a function of bias voltage, tip-sample distance and photon energy.

Finally, we propose a simple model to study the problem of light rectification when the tip is placed over an adsorbed molecule with a characteristic vibrational mode. The use of the Keldysh formalism allows us to obtain the contribution to the currents from the main inelastic processes where one phonon is emitted and reabsorbed during tunnelling.

The rest of the paper is organized as follows: in the next section the model is presented and it is shown how the coupling with the external field may be written in a tight-binding form. The third section is devoted to the formulation of the problem in terms of non-equilibrium Green's function. An outline is given of a procedure that allows us to find the induced currents at any desired order in the external field. In the fourth section we give the expressions for the signal generated by mixing two frequencies and for the rectified current when a DC bias is applied. Different limiting cases are analysed. Some numerical results for a system modelling a tungsten tip and a graphite sample are given and discussed in section five. The model calculations for the rectified current in the presence of an adsorbate are presented in section six and the paper ends with some concluding remarks.

2. Description of the laser field and effective tip-sample coupling

We represent the tip by a metallic sphere of radius R with a small protrusion including a few atoms as shown in figure 1. This protrusion establishes the electrical contact with the sample but its effect on the EM field at the interface is neglected.

Upon these conditions it is found [9] that the incident field normal to the sample surface is enhanced in the gap region by a factor of order R/D , where D is measured as shown in figure 1.

Without loss of generality we may assume that the tunnelling currents are localized between two atoms: one at the tip of the protrusion and the other on

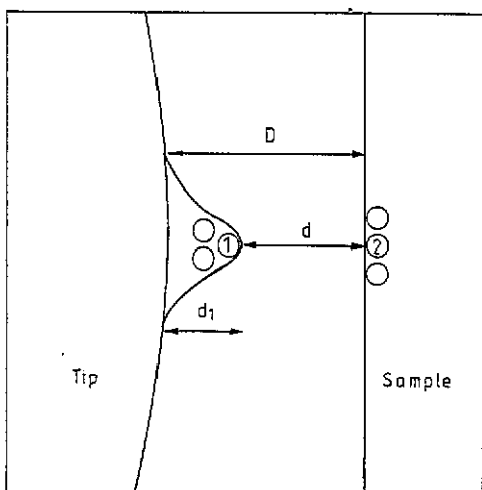


Figure 1. Model geometry for the tip-sample interface used in our calculations.

the sample surface. In the absence of any external field our system is described by the Hamiltonian

$$H = H_S + H_T + T_{12}^0 \sum_{\sigma} (c_{1\sigma}^{\dagger} c_{2\sigma} + c_{2\sigma}^{\dagger} c_{1\sigma}) \quad (1)$$

where $c_{i\sigma}^{\dagger}$ creates an electron with spin σ at site i ($i = 1$ refers to the tip site and $i = 2$ refers to the sample site). H_T and H_S describe the motion of electrons on the isolated tip and sample respectively.

The EM field is then introduced by means of a vector potential \mathbf{A} . In the tight-binding approximation the interaction with a vector potential may be completely taken into account by a phase factor affecting the hopping elements only. To show this we start with the expression

$$\delta H = -\frac{1}{c} \int J(\mathbf{r}) \delta \mathbf{A}(\mathbf{r}) d^3 r \quad (2)$$

which gives the change in the Hamiltonian due to a small change in the vector potential. Here $J(\mathbf{r})$ is the density current operator. In a tight-binding approximation J is related to the hopping elements and equation (2) may be written as

$$\delta H = -\frac{ie}{\hbar c} \sum_{j k \sigma} \left(T_{j k} c_{k\sigma}^{\dagger} c_{j\sigma} - T_{k j} c_{j\sigma}^{\dagger} c_{k\sigma} \right) \int_{\mathbf{r}_j}^{\mathbf{r}_k} \delta \mathbf{A} d\mathbf{l}. \quad (3)$$

This equation can now be integrated to obtain the form of the hopping elements in the presence of an external field

$$T_{j k} = T_{j k}^0 \exp \left(-\frac{ie}{\hbar c} \int_{\mathbf{r}_j}^{\mathbf{r}_k} \mathbf{A} d\mathbf{l} \right) = T_{k j}^*. \quad (4)$$

Let us remark that this expression is valid even for a time-dependent field. Also note that this formulation is gauge-invariant: a unitary transformation can always be found leading from a shift in the site energies into a time-dependent phase in the

hopping elements. This is equivalent to a gauge transformation that removes the scalar potential.

For the case of a single connection between tip and sample we have

$$T_{12} = T_{12}^0 \exp\left(\frac{ie}{\hbar c} \bar{A}(t)d\right) = T_{21}^*$$

where $\bar{A}(t) = A_0 \cos(\omega_0 t)$ is the typical amplitude of the field at the gap region between atoms 1 and 2 and d is the tip-sample distance as shown in figure 1.

The coupling with the external field is controlled by the parameter $\alpha_0 = eA_0d/\hbar c = eE_0d/\hbar\omega_0$, which is much smaller than 1 for most cases of interest. It is then possible to expand T_{12} as

$$T_{12} = T_{12}^0 \left(1 + i\alpha_0 \cos(\omega_0 t) - \frac{\alpha_0^2}{2} \cos^2(\omega_0 t) + \dots \right)$$

and keep only the terms that give rise to the non-linear effects that one is interested in. In I we have restricted ourselves to the first two terms in this expansion. This is enough to obtain the rectified current up to second order when the applied bias is zero. Here we have to go beyond this approximation and include also the quadratic term in α_0 in order to obtain the response when a non-zero tip-sample bias is applied.

For the case of the difference frequency generation we must consider $\bar{A}(t) = A_1 \cos(\omega_1 t) + A_2 \cos(\omega_2 t)$. However, for the sake of simplicity, the most general discussion given in the next section corresponds to the case of a single laser at a frequency ω_0 .

3. Induced currents in terms of Green's functions

In this section we briefly discuss the Green's function formalism used to analyse the present non-equilibrium problem. In this formalism, in addition to the usual retarded (G^r) and advanced (G^a) Green's functions, another correlation function denoted by G^{+-} is needed [10]. It is defined as

$$G_{jk\sigma}^{+-}(t, t') = i\langle c_{k\sigma}^\dagger(t') c_{j\sigma}(t) \rangle$$

where the angle brackets imply here averaging over available states for the system which is out of equilibrium. One of the advantages of this formalism is that the current between sites 1 and 2 can be obtained from the equation

$$I(t) = \frac{e}{\hbar} \sum_{\sigma} (T_{12}(t) G_{21\sigma}^{+-}(t, t) - T_{21}(t) G_{12\sigma}^{+-}(t, t)). \quad (4)$$

The different Green's functions of this problem satisfy the following set of coupled integral equations:

$$\begin{aligned} G^{r,a}(t, t') &= g^{r,a}(t, t') + \int_{-\infty}^{\infty} dt_1 G^{r,a}(t, t_1) V(t_1) g^{r,a}(t_1, t') \\ G^{+-}(t, t') &= \int_{-\infty}^{\infty} dt_1 dt_2 [\delta(t - t_1) + G^r(t, t_1) V(t_1)] g^{+-}(t_1, t_2) \\ &\quad \times [\delta(t_2 - t') + V(t_2) G^r(t_2, t')] \end{aligned} \quad (5)$$

where the perturbation $V(t)$ is taken as the effective time-dependent coupling between tip and sample, and g corresponds to the unperturbed system in which both tip and sample are in thermodynamic equilibrium with chemical potentials μ_1 and μ_2 respectively. The applied bias $V = \mu_1 - \mu_2$ is assumed to produce a rigid shift of the unperturbed bands.

In order to solve equation (5) it is convenient to Fourier transform the variable $t - t'$ into the frequency w . Then, if we call $\tau = (t + t')/2$, all Green's functions may be expanded as

$$G(\tau, w) = \sum_{n=-\infty}^{\infty} \exp(inw_0\tau) G_n(w) \quad (6)$$

Then, Dyson's equation for the retarded and advanced Green's functions is transformed into a set of linear algebraic equations in the Fourier components G_n that can be easily solved by truncation at a given finite order [7].

The current given by equation (4) will also be expressed as a Fourier series. The components I_n are complex quantities which satisfy the condition $I_{-n} = I_n^*$. These are formally given by

$$I_n = \frac{2e}{h} \int_{-\infty}^{\infty} dw \sum_{l+l'=n} \{ g_1^r(w + \frac{1}{2}n w_0) [(D_{12}^r)_l(w + \frac{1}{2}l' w_0) \\ g_2^{+-}(w + \frac{1}{2}(l' - l) w_0)(D_{21}^a)_{l'}(w - \frac{1}{2}l w_0)] \\ - [(D_{12}^r)_l(w + \frac{1}{2}l' w_0) g_2^{+-}(w + \frac{1}{2}(l' - l) w_0)(D_{21}^a)_{l'}(w - \frac{1}{2}l w_0)] \\ \times g_1^a(w - \frac{1}{2}n w_0) + [(D_{21}^r)_l(w + \frac{1}{2}l' w_0) g_1^{+-}(w + \frac{1}{2}(l' - l) w_0) \\ \times (D_{12}^a)_{l'}(w - \frac{1}{2}l w_0)] g_2^a(w - \frac{1}{2}n w_0) - g_2^r(w + \frac{1}{2}n w_0) \\ \times [(D_{21}^r)_l(w + \frac{1}{2}l' w_0) g_1^{+-}(w + \frac{1}{2}(l' - l) w_0)(D_{12}^a)_{l'}(w - \frac{1}{2}l w_0)] \} \quad (7)$$

where $D^{r,a} = V + V G^{r,a} V$ (integration over internal times is implicitly assumed).

Equation (7) is the starting point for calculating the induced currents at any desired order in the external field. Notice that the problem is reduced to obtaining the components $(D_{j,k}^{r,a})_l$, which in turn can be obtained from the Green's functions components $(G_{j,k}^{r,a})_l$.

4. Difference frequency generation and rectified current

When there are two fields of frequencies ω_1 and ω_2 at the microscope interface, all Fourier transformed quantities like the Green's functions G defined in the previous section have components G_{n_1, n_2} , where the subindexes n_1 and n_2 refer to the order of expansion in the frequencies ω_1 and ω_2 , respectively. The signal emitted at the difference frequency $\omega_1 - \omega_2$ is proportional to the current component $I_{1,-1}$.

Keeping terms up to second order in the field we obtain the following expression for $I_{1,-1}$:

$$I_{1,-1} = \frac{e\alpha_1\alpha_2(T_{12}^0)^2}{4\hbar} \int_{-\infty}^{\infty} dw \Sigma^r(w + \Delta) \Sigma^a(w - \Delta)$$

$$\begin{aligned}
& \times \{ [\gamma_2^1(w, \Delta, \bar{w}) + (\delta^r(w, \Delta, \bar{w}) + \beta^r(w, \Delta)) g_2^{+-}(w + \Delta) \\
& + (\delta^a(w, -\Delta, \bar{w}) + \beta^a(w, -\Delta)) g_2^{+-}(w - \Delta)] \\
& \times (g_1^r(w + \Delta) - g_1^a(w - \Delta)) \\
& + [\gamma_1^2(w, \Delta, \bar{w}) + (\delta^r(w, -\Delta, \bar{w}) + \beta^r(w, -\Delta)) g_1^{+-}(w - \Delta) \\
& + (\delta^a(w, \Delta, \bar{w}) + \beta^a(w, \Delta)) g_1^{+-}(w + \Delta)] (g_2^a(w - \Delta) \\
& - g_2^r(w - \Delta)) + (\bar{w} \rightarrow -\bar{w}) \}
\end{aligned} \tag{8}$$

where

$$\Delta = \frac{1}{2}(w_1 - w_2)$$

$$\bar{w} = \frac{1}{2}(w_1 + w_2)$$

$$\Sigma^{r,a}(w) = [1 - (T_{12}^0)^2 g_1^{r,a}(w) g_2^{r,a}(w)]^{-1}$$

$$\beta^{r,a}(w, \Delta) = -\frac{1}{2} T_{12}^0 \Sigma^{r,a}(w - \Delta) (1 + (T_{12}^0)^2 g_2^{r,a}(w + \Delta) g_1^{r,a}(w - \Delta))$$

$$\begin{aligned}
\gamma_j^k(w, \Delta, \bar{w}) = & (1 - (T_{12}^0)^2 g_j^r(w + \Delta) g_k^r(w + \bar{w})) |\Sigma(w + \bar{w})|^2 \\
& \times (1 - (T_{12}^0)^2 g_j^a(w - \Delta) g_k^a(w + \bar{w})) g_j^{+-}(w + \bar{w})
\end{aligned}$$

$$\begin{aligned}
\delta^{r,a}(w, \Delta, \bar{w}) = & (T_{12}^0)^2 \Sigma^{r,a}(w + \bar{w}) [\Sigma^{r,a}(w - \Delta) (g_2^{r,a}(w + \Delta) g_1^{r,a}(w + \bar{w}) \\
& + g_1^{r,a}(w - \Delta) g_2^{r,a}(w + \bar{w})) + 2\beta^{r,a}(w, \Delta) g_1^{r,a}(w + \bar{w}) g_2^{r,a}(w + \bar{w})]
\end{aligned}$$

In the limit $\Delta \rightarrow 0$ and for $\alpha_1 = \alpha_2 = \alpha_0$, $I_{1,-1}$ reduces to the rectified current I_0 that takes a much simpler form. At zero temperature I_0 is given by

$$\begin{aligned}
I_0 = & \frac{e\alpha_0^2(T_{12}^0)^2}{\hbar} \left[\int_{\mu}^{\mu+eV+w_0} dw F_1(w, -w_0) \right. \\
& \left. + \int_{\mu}^{\mu+eV-w_0} dw F_1(w, w_0) + 2 \int_{\mu}^{\mu+eV} dw F_2(w) \right]
\end{aligned} \tag{9}$$

where

$$\begin{aligned}
F_1(w, w_0) = & |\Sigma^r(w) \Sigma^r(w + w_0)|^2 |1 - (T_{12}^0)^2 g_1^r(w + w_0) g_2^r(w)|^2 \\
& \times \text{Im}(g_2^a(w + w_0)) \text{Im}(g_1^a(w))
\end{aligned}$$

$$\begin{aligned}
F_2(w) = & |\Sigma^r(w)|^2 \text{Re}(\delta^r(w, w_0, 0) + \delta^r(w, -w_0, 0) + 2\beta(w, 0)) \\
& \times \text{Im}(g_2^a(w)) \text{Im}(g_1^a(w))
\end{aligned}$$

This expression reduces to that obtained in I for $V = 0$.

It is important to note that $I_{1,-1}$ does not have any singular behaviour when $\Delta \rightarrow 0$. Some recent experimental data [3] indicate that the difference frequency signal behaves as Δ^{-1} for Δ in the range from 1 to 100 MHz. This behaviour cannot be explained within our model and must be related to the coupling with surface vibrational modes of extremely low frequencies [1].

Notice that in the experiments of [1] $\Delta \leq 100$ MHz is such a small photon energy ($\leq 10^{-4}$ meV) that in this regime we can approximate $I_{1,-1}$ to a good accuracy by I_0 . Within this limit, the power emitted in the difference frequency is a measure of I_0^2 . From the experimental point of view, measuring the emitted radiation may be

simpler than measuring the rectified current, since the latter must be subtracted from the normal tunnelling current.

Another important point is that we can show from equation (9) that I_0 in the limit $w_0 \rightarrow 0$ is proportional to the second derivative of the static I - V curve, i.e. we can show that [3]

$$\lim_{w_0 \rightarrow 0} I_0 = (eE_0d)^2 \left(\frac{\partial^2 I^{\text{DC}}}{\partial V^2} \right).$$

This can be easily checked by considering the limit of large tip-sample distances, where an expansion up to second order in the hopping T_{12} yields

$$I_0 = \alpha_0^2 [I^{\text{DC}}(V + w_0) + I^{\text{DC}}(V - w_0) - 2I^{\text{DC}}(V)] \quad (10)$$

where

$$I^{\text{DC}}(V) \simeq \frac{e(T_{12}^0)^2}{h} \int_{\mu}^{\mu+V} dw \text{Im}(g_2^s(w)) \text{Im}(g_1^s(w))$$

Equation (10) is just the three-point approximation to the second-order derivative that gives the previously mentioned result in the limit $w_0 \rightarrow 0$. This is the physically expected result [3]: in the limit of very low frequencies the system follows adiabatically to the external perturbation and thus the dynamic response can be derived from the static (non-linear) response.

An equation like (10) has been used by Wingreen [11] to analyse the problem of frequency response in double-barrier structures. This result may also be obtained from our formulation if a central site with a time-dependent site energy is considered and the energy dependence of the density of states DOS of the left and right electrodes is neglected. Our result for the rectified current (equation 9) is more general as it takes into account the full energy dependence in the propagators.

5. Some results for a model graphite surface

Many experiments on STM with laser radiation have been performed on graphite samples. It is thus desirable to perform calculations for this particular system.

As in a previous work [12], we describe the electronic structure of a graphite surface by a tight-binding Hamiltonian on a hexagonal lattice with one orbital per site. The hopping elements between first neighbours are fitted in order to give the band width of *ab initio* calculations [13]. Using the recursion method [14] with more than 200 levels in the continued fraction, we obtain the smooth surface electronic DOS that is shown in figure 2. This is in reasonable agreement with more sophisticated calculations.

On the other hand, we represent the tip electronic structure by a semi-elliptical band with a total width of 16 eV, filled up to 1.25 electrons; this corresponds to the number of sp electrons in tungsten. The hopping integral between tip and sample atoms may be fitted by [12]

$$T_{12}^0 = T_0 \left(\frac{d_0}{d + d_0} \right)^2 e^{-\alpha d}$$

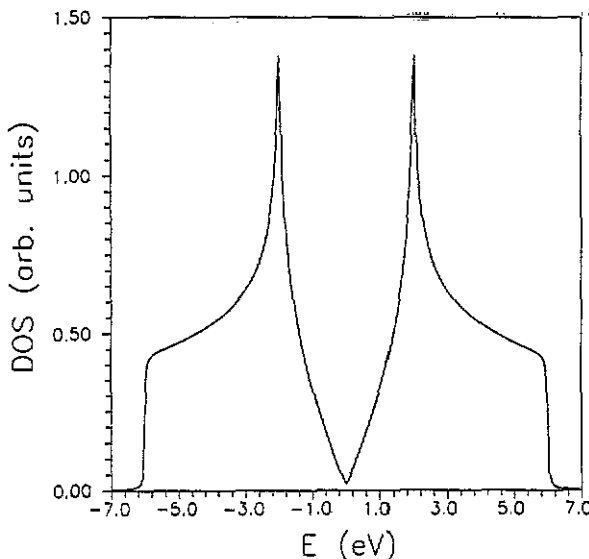


Figure 2. Model electronic density of states for graphite obtained for a hexagonal lattice with one orbital per site using the recursion method up to 300 pairs of coefficients in the continued fraction expansion of the Green's functions.

where d_0 is the close contact distance, taken as 2.5 \AA , $T_0 \simeq 1.2\text{ eV}$ and $\alpha = 0.58\text{ \AA}^{-1}$.

We shall concentrate on the behaviour of the rectified current as a function of bias voltage, tip-sample distance and photon energy. As mentioned above, the following results also hold for $I_{1,-1}$ when $\Delta = (\omega_1 - \omega_2)/2$ is small enough; this is indeed the case for the available experimental data.

In order to compare with experimental results we show in figure 3 our calculations for both the static current-voltage characteristic and the rectified current as a function of bias voltage for different tip-sample distances. In agreement with the experimental results the I - V curves show a nonlinear rise. The rectified current has a clear peak for a bias voltage of $\simeq 2\text{ V}$, corresponding to the peak in the graphite DOS. Unfortunately the peak region has not been analysed in the experimental data of [4].

When the tip-sample distance is reduced but is still larger than $\simeq 4.5\text{ \AA}$ the rectified current increases. However, as shown in figure 4, this behaviour is not monotonic. As already noted in I, the rectified current has a maximum for a tip-sample distance almost 2 \AA larger than the close-contact distance. It can be observed from the curves in figure 4 that the maximum position slightly displaces to larger distances when the bias voltage is increased. On the other hand, as the output rectified signal increased with the applied voltage, a large enough DC bias could help in the experimental detection of this maximum.

It is interesting to explore with our model the departure from the adiabatic response. In figure 5 the rectified current is plotted against bias voltage for different photon energies: 0.1 , 0.2 and 0.3 eV . Note that for the CO_2 lasers used in experiments of [4] $\hbar\omega_0 \simeq 128\text{ meV}$. The second derivative of the static I - V curve is also shown for comparison. This has been obtained using a finite difference scheme with a voltage step of 5 mV .

As can be observed, the agreement between I_0 and its adiabatic approximation at higher photon energies is poorer in the peak region. The effect of a finite photon energy is to smear out the structure on a scale given by $\hbar\omega_0$, and thus any structure in the I - V curve on a smaller scale may be completely washed out.

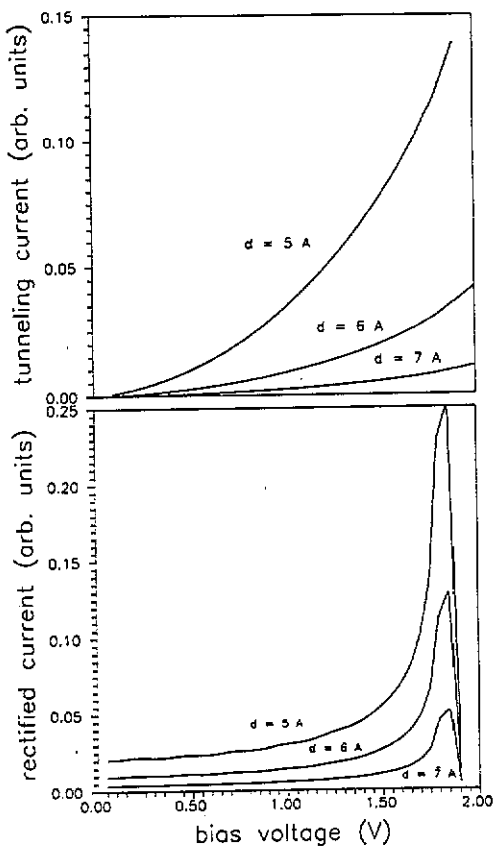


Figure 3. Tunnelling current and rectified current as a function of bias voltage for three different tip-sample distances and for $\hbar\omega_0 = 0.1$ eV.

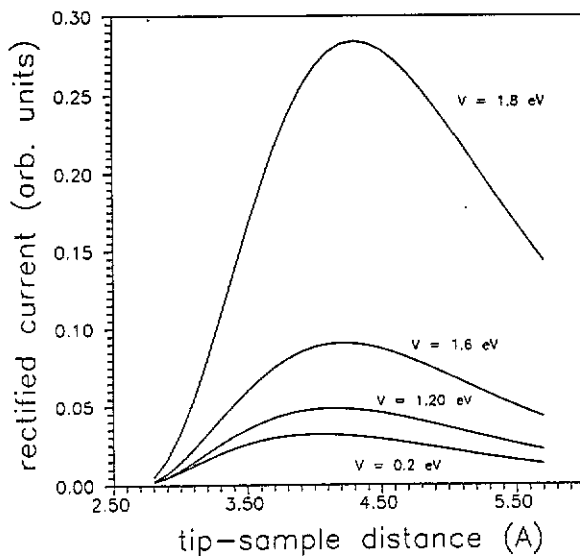


Figure 4. Rectified current I_0 as a function of the tip-sample distance d for various values of the applied bias.

6. Rectified current in the presence of an adsorbed molecule

The relation between the rectified current and the second derivative of the

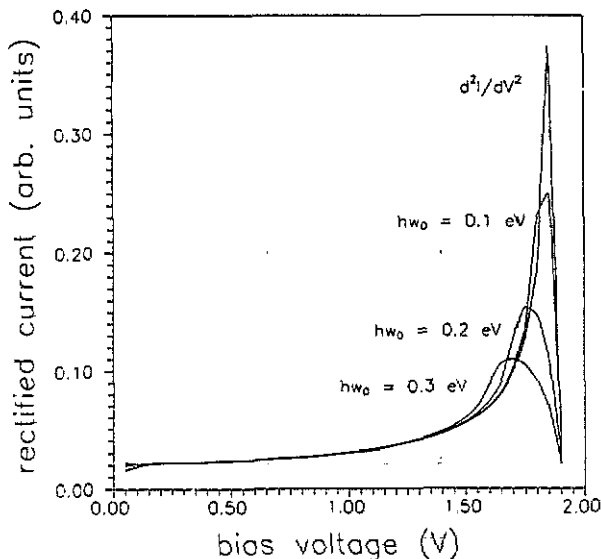


Figure 5. Rectified current for three different photon energies: 0.1, 0.2 and 0.3 eV. The adiabatic approximation to I_0 is also plotted for comparison.

characteristic curve discussed in the previous sections, suggests that I_0 should be particularly affected by the coupling of the tunnelling electrons with the localized vibrations of adsorbed molecules. The opening of an inelastic channel for tunnelling must be reflected as a peak in the rectified current. Calculations based on a classical polarizability picture for the rectified current in the presence of large adsorbate molecules has recently been presented by Molotkov [15]. Here we concentrate on the case of small molecules at low temperature that must be analysed by a full quantum mechanical description.

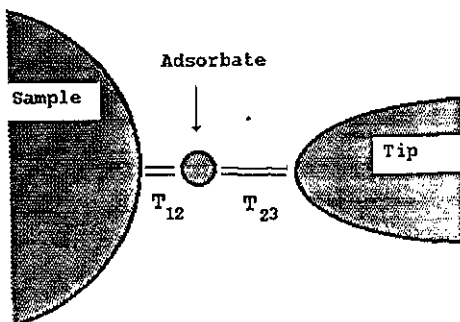


Figure 6. Schematic drawing of the model considered to study the photoinduced currents in the presence of an adsorbed molecule.

In order to describe this situation we consider a simplified model as depicted in figure 6. The adsorbate is characterized by a vibrational mode of frequency ω_p and has an electronic resonant level at ϵ_2 . This system is described by the Hamiltonian

$$H = H_T + H_S + T_{12}(c_{1\sigma}^\dagger c_{2\sigma} + c_{2\sigma}^\dagger c_{1\sigma}) + T_{23}c_{2\sigma}^\dagger c_{3\sigma} \\ + T_{32}c_{3\sigma}^\dagger c_{2\sigma} + \epsilon_2 c_{2\sigma}^\dagger c_{2\sigma} + \hbar\omega_p a^\dagger a + \lambda(a + a^\dagger)c_{2\sigma}^\dagger c_{2\sigma}$$

where a^\dagger and a are boson operators for the vibrational mode, T_{23} and T_{12} are the hopping elements connecting the adsorbate with, respectively, the tip and the sample. The term in λ describes the coupling between local phonons and charge excitations on the adsorbate. A similar model has been considered by Persson and Baratoff [16]. Here, the interaction with the laser field is taken into account by $T_{23}(t)$.

If we assume that T_{23} is small enough ($T_{23} \ll T_{12}$), we can approximate I_0 by equation (10). The problem is then reduced to obtaining an expression for I_{DC} in the presence of the adsorbate's vibrational mode. Using the Keldysh formalism and keeping contributions up to second order in λ [17] (details will be given elsewhere) it can be shown that I_{DC} decouples into an *elastic* part, given at zero temperature by

$$I_{\text{el}}^{\text{DC}} = k \int_{\mu}^{\mu+eV} dw |G_{22}^r(w)|^2 \text{Im } g_1^a(w) \text{Im } g_3^a(w) \quad (11)$$

and an *inelastic* part given by

$$I_{\text{in}}^{\text{DC}} = k \lambda^2 \int_{\mu}^{\mu+eV-\hbar w_p} dw |G_{22}^{r(0)}(w + w_p) G_{22}^{r(0)}(w)|^2 \text{Im } g_1^a(w) \text{Im } g_3^a(w + w_p) \quad (12)$$

where $k = e(\alpha_0 T_{12} T_{23}^0)^2 / h$. $G_{22}^{r(0)}$ in equation (12) is the retarded Green's function for zero electron-phonon coupling. An explicit expression for $I_{\text{el}}^{\text{DC}}$ at second order in λ is obtained by replacing G_{22}^r in equation (11) by

$$G_{22}^{r(0)} + G_{22}^{r(0)} \Sigma_{22}^r G_{22}^{r(0)}$$

Then, neglecting the real part in Σ_{22}^r (this is valid because the imaginary part contains the most singular contribution [17]), we obtain

$$I_{\text{el}}^{\text{DC}} = I_{\text{el}}^{\text{DC}(0)} + I_{\text{el}}^{\text{DC}(2)} \quad (13)$$

where

$$I_{\text{el}}^{\text{DC}(2)} = -2k\lambda^2 \int_{\mu}^{\mu+eV-\hbar w_p} dw |G_{22}^{r(0)}(w + w_p)|^2 \text{Im } G_{22}^{a(0)}(w) \times G_{22}^{a(0)}(w + w_p) \text{Im } g_1^a(w) \text{Im } g_3^a(w). \quad (14)$$

The terms $I_{\text{el}}^{\text{DC}(2)}$ and $I_{\text{in}}^{\text{DC}}$ yield the phonon effects up to second order in λ . Let us analyse these expressions for the case where the energy dependence of $\text{Im}(g_1^a)$ and $\text{Im}(g_3^a)$ can be neglected. All the integrands are then determined by the form of $G_{22}^{r(0)}(w)$ that can be approximated by a Lorentzian [16]:

$$G_{22}^{a(0)}(w) = \frac{1}{w - \epsilon_2 - i\Gamma}.$$

The width $\Gamma = T_{12}^2 \text{Im}(g_1^a)$ is of the order of 1 eV for a chemisorbed molecule on a metal surface. This implies that the presence of the adsorbate modifies the tunnelling current only if the resonant level lies a few eV from the Fermi energy.

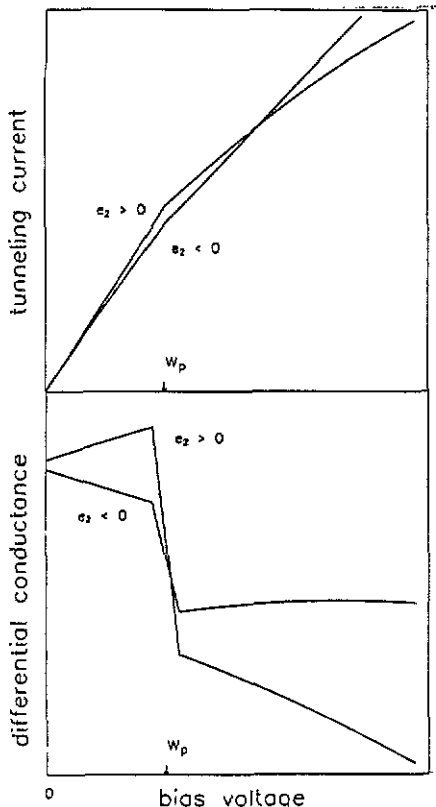


Figure 7. Schematic representation of the tunnelling current and its first derivative in the presence of an adsorbed molecule. $\epsilon_2 > 0$ and $\epsilon_2 < 0$ correspond to the case of a resonant level above and below the Fermi energy, respectively.

On the other hand, both the inelastic contribution I_{in}^{DC} and the contribution $I_{el}^{DC(2)}$ differ from zero only when $|eV| \geq \hbar w_p$, i.e. when the tunnelling electrons have enough energy to emit one phonon. $I_{el}^{DC(2)}$ takes into account those (virtual) processes in which the emitted phonon is readSORBED during tunnelling. The present approach does not include the possibility of multiphonon processes of higher order in λ .

Before analysing the rectified current it is instructive to look at the effect of the adsorbate on the normal tunnelling current and its first derivative. Figure 7 shows a schematic representation of the typical behaviour that can be found for both $\epsilon_2 < 0$ and $\epsilon_2 > 0$, assuming that $\mu = 0$ and $|\epsilon_2 + \hbar w_p| \leq \Gamma$. We have chosen the relation λ/Γ to be arbitrarily large in order to have a clear view of the qualitative behaviour. It can be observed that in both cases there is a decrease in the conductance when resonant tunnelling via the vibrational mode is activated [16]. This is due to the negative contribution $I_{el}^{DC(2)}$ that is larger than I_{in}^{DC} . The background conductance related to $I_{el}^{DC(0)}$ increases with bias for $V \leq \epsilon_2$ and decreases in the reverse case.

This qualitative discussion shows that the rectified current, which is essentially given by the second derivative of the tunnelling current (equation (10)), will be characterized by a negative or positive background depending on the relation between ϵ_2 and V , and by an inverted peak at $V = \hbar w_p$. If the experiments are performed using the difference frequency generation effect, the onset of inelastic tunnelling will be reflected as a positive peak in the emitted power when $\epsilon_2 < 0$ or as an inverted

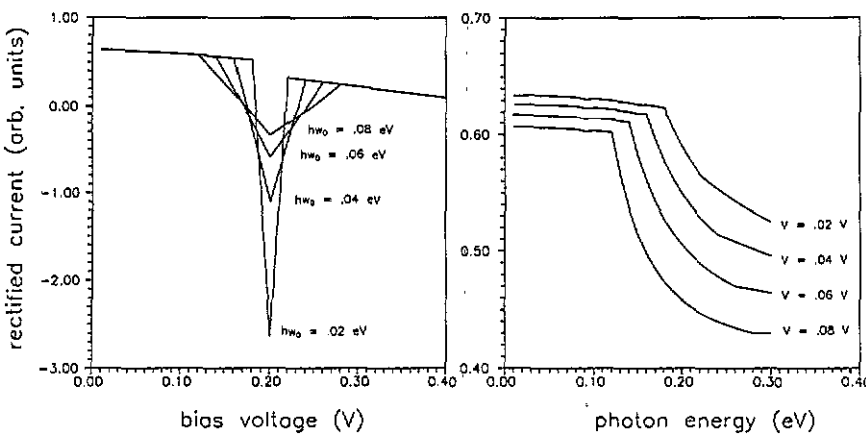


Figure 8. Rectified current in the presence of an adsorbed molecule with a vibrational mode at $\hbar\omega_p = 0.2$ eV as a function of bias voltage and photon energy.

peak, or even an inverted double peak, when $\epsilon_2 > 0$.

The curves in figure 8 show the behaviour of the rectified current in the presence of the adsorbate as a function of both the bias voltage and the photon energy. For this example we have chosen $\epsilon_2 = 0.50$ eV, $\hbar\omega_p = 0.20$ eV and $(\lambda/\Gamma)^2 = 0.1$ in order to represent the stretching mode of a small molecule like CO or NO adsorbed on a metal surface [18].

The width of the peak in I_0 as a function of bias is determined by $\hbar\omega_0$; its intensity decreases as $(\hbar\omega_0)^{-1}$, in agreement with equation (10). It can be seen that I_0 may even change its sign when the photon energy is not very large. I_0 as a function of photon energy exhibits a sharp drop at $\hbar\omega_0 \simeq \hbar\omega_p - eV$. This drop is more pronounced for increasing bias voltage.

It is worth mentioning that varying ϵ_2 can modify the peak height and the rectified current background as discussed above but the qualitative shape of the curves remains unchanged. As expected, the peak intensity reduces when Γ is increased.

7. Concluding remarks

In the present work we have extended the theoretical approach reported in I in many different aspects. First, the inclusion of higher-order terms in the coupling with the laser field has made it possible to consider the induced photocurrents for the case where a direct bias is applied. We have obtained closed expressions for the difference frequency signal and for the rectified current and showed how they reduce to the adiabatic response in the limit of very small frequencies. Second, model calculations for a graphite sample have been presented as an attempt to make contact with recent experimental data. Finally, we have proposed a model to describe the induced currents in the presence of an adsorbed molecule which can be used to analyse future experimental results [19] in this field.

Regarding the problem of the frequency limits for the dynamical response in STM, our model suggests that there is no clear cut-off except for photon energies comparable to the total electronic band widths. Obviously, the assumption of perfect screening as discussed in our model [7] for the coupling with the EM field breaks

down at lower frequencies, in the region of surface plasmons [20]. Thus, it is not the electron tunnelling time but rather the EM coupling which limits the dynamical response.

In conclusion we believe that, in spite of its simplicity, our approach can account for many different phenomena related to laser induced tunnelling in STM and can also be applied to study the same problem in double-barrier structures. It has also some advantages over other theories recently proposed [21] based on the transfer Hamiltonian method. The main advantage is that the use of the Keldysh formalism provides a direct way to obtain the induced currents and to include many-body effects like electron-phonon or electron-electron interactions. On the other hand, the combination of the Keldysh formalism and tight-binding representation is a useful scheme for taking into account the local electronic properties that are relevant in a description of the main physical effects in such systems.

Acknowledgments

One of us (ALY) would like to thank Ministerio de Educación y Ciencia de España for financial support. This work was partially supported by the CICYT under contract MAT 89-165.

References

- [1] Arnold L, Krieger W and Walther H 1987 *Appl. Phys. Lett.* **51** 786
- [2] Hamers R J and Cahill D G 1990 *Appl. Phys. Lett.* **57** 2031
- [3] Krieger W, Suzuki T, Volcker M and Walther H 1990 *Phys. Rev. B* **41** 10229
- [4] Volcker M, Krieger W and Walther H 1991 *Phys. Rev. Lett.* **66** 1717
- [5] Cutler P H, Feuchtwang T E, Tsong T T, Nguyen H and Lucas A A 1987 *Phys. Rev. B* **35** 7774
- [6] Buttiker M and Landauer R 1986 *IBM J. Res. Dev.* **30** 451
- [7] Levy Yeyati A and Flores F 1991 *Phys. Rev. B* **44** 9020
- [8] Keldysh L V 1965 *Sov. Phys.-JETP* **20** 1018
- [9] Johansson P, Monreal R and Apell P 1990 *Phys. Rev. B* **42** 9210
- [10] Caroli C, Combescot R, Nozieres P and Saint-James D 1971 *J. Phys. C: Solid State Phys.* **4** 916
- [11] Wingreen N S 1990 *Appl. Phys. Lett.* **56** 253
- [12] Levy Yeyati A and Flores F 1992 *Ultramicroscopy* submitted
- [13] Tatar R C and Rabii S 1982 *Phys. Rev. B* **25** 4126
- [14] For a review, see
Haydock R 1981 *Excitations in Disordered Systems* ed M F Thorpe (New York: Plenum)
- [15] Molotkov S N 1991 *JETP Lett.* **54** 481
- [16] B. Persson N J and Baratoff A 1987 *Phys. Rev. Lett.* **59** 339
- [17] The treatment used here is based on that proposed by
Anda E V and Flores F 1991 *J. Phys.: Condens. Matter* **3** 9087
- [18] Stohr J and Jaeger R 1982 *Phys. Rev. B* **26** 4111
- [19] Lovric D and Gummel B 1988 *Phys. Rev. B* **38** 10323
- [20] Zangwill A 1988 *Physics at Surfaces* (Cambridge: Cambridge University Press)
- [21] Apell S P and Penn D R 1992 *Phys. Rev. B* **45** 6757